Conference Proceedings of 5th International Conference on Countermeasures to Urban Heat Islands (IC2UHI) 2019
December 2-4, 2019, Hyderabad, India
https://doi.org/10.37285/bsp.ic2uhi.17

A pavement-watering thermal model validation for SOLENE-microclimat: application to the Buire street

Marie-Hélène Azam, Univ. Nantes, CNRS UMR 6183, GeM, Nantes, France
Auline Rodler[1], Cerema, Equipe-Projet BPE, F-44000, Nantes, France
Marjorie Musy, Cerema, Equipe-Projet BPE, F-44000, Nantes, France
Benjamin Morille, Soleneos, France
Sihem Guernouti, Cerema, Equipe-Projet BPE, F-44000, Nantes, France

ABSTRACT

Pavement watering is considered as a solution to mitigate the Urban Heat Island, particularly for compact urban areas. This technique has been mainly studied through experimental works and its impact on urban energy balance at the microscale has rarely been addressed by modeling. A thermal soil model dedicated to pavement watering has been developed within the urban climate model SOLENE-Microclimat. Watering events are modeled through a runoff convective heat flux and a latent heat flux. This watering model is presented here and applied to the Buire street, in the city center of Lyon (France). The model performances are assessed on two hot, clear and sunny days. Simulated and measured *in-situ* surface temperatures as well as radiation measurements are compared. A RMSE of 2.99°C is observed. Modeling such a complex environment requires multiple input data which are not always available. The influence of using non-local data and thus neglecting the UHI effect on the soil temperature is studied. It leads to an underestimation of the surface temperature by 0.93°C. Finally, the effect of pavement watering on soil temperature is evaluated. Evening watering scenario (17h to 22h GMT) decreases the surface temperature by 4.09 °C.

Introduction

Reducing the urban heat island (UHI) effect has become a challenge for the technical and scientific community. For that purpose, several countermeasures are investigated for various regions and climates. In dense urban areas, one of the solutions to mitigate the UHI consists in spreading water over paved areas. Several techniques can be used: cleaning trucks, spray nozzles in the pavement. Under warm conditions, they provide a quick answer to high ground surface temperatures, first contributing to cool the surface temperatures and then the air temperature.

Watering has been mainly studied through experimental works (Hendel and Royon 2015). Its efficiency has been proven under warm conditions. Takahashi et al. (2010) have shown that it can reduce the air temperature by 4°C in the afternoon.

However, this solution has rarely been modeled. To the best of our knowledge only Town Energy Balance (TEB) model is able to simulate pavement watering events at mesoscale (Broadbent et al. 2017). In previous works, a pavement watering model has been developed in the micro-scale simulation tool SOLENE-Microclimat (Azam, Bernard, et al. 2018). Watering events are modeled through a runoff convective heat flux and a latent heat flux.

[1] Corresponding Author: [auline.rodler@cerema.fr], [+332 40 12 83 19].

This pavement watering model has been evaluated on an open-space area, a parking-lot. It is now applied to a complex urban scene to evaluate it under these conditions.

For that purpose, the Buire street, in the city center of Lyon (France), is modeled with SOLENE-Microclimat. It has been equipped by Veolia 2EI with a watering device, consisting of sprinklers located in the curbside (Fig. 2). An experimental campaign has been carried out by Veolia 2EI to evaluate the impact of those waterings, including different scenarios. In this paper, we aim to evaluate the model behavior by comparing the *in-situ* measured pavement temperatures to the results of the simulations.

Modeling such a complex environment needs multiple data, in particular the materials properties and local meteorological data. They are usually not accessible for the user of the model. Local meteorological data are important to take into account local phenomenon as the UHI. We will assess the error on the pavement temperature due to the use of reference meteorological data instead of local data. Finally, the influence of the watering practice is quantified in the Buire street by comparing simulations with and without waterings.

Materials and method

SOLENE-microclimat pavement watering model is briefly presented here. Then, the considered case study and the different hypothesis made are detailed. SOLENE-microclimat improved soil model is used described in (Azam, Morille, et al. 2018). The watering events affecting the surface energy balance of the soil model are described below.

Surface energy balance

Usually, the surface energy balance of a dry surface is composed of three heat fluxes: the net radiative heat flux (R_{net}), the conductive heat flux (Q_{cond}) and the sensible heat flux. In order to model a watering event, several additional heat fluxes are considered. The water spread over a surface can either infiltrate in the soil, runoff, or evaporate. For each of those paths, the surface energy budget should be adapted.

The soil model used here has been designed for impervious surface. The portion of water that infiltrates in the soil is supposed negligible compared to the one that runs-off and evaporates. Only runoff and evaporation are thus considered and two additional heat fluxes are taken into account. While the water runoff over the surface, a convective heat flux density ($Q_{wat-pav}$) is exchanged between the soil surface and the water spread. Meanwhile, a part of the water evaporates, leading to a latent heat flux (LE). Eq. (1) describes the resulting surface energy balance. The method and equations used to calculate each heat flux are described hereafter.

$$R_{net} = Q_{cond} + h_c \left(T_{surf} - T_{air}\right) + Q_{wat-pav} + LE \quad (1)$$

Net radiative heat flux. It is calculated using Eq. (2), considering the short-wave incident radiation R_{sun}, long-wave radiative budget of the soil surface with the surrounding ones noted $R_{IR,Urb}$ and with the net sky noted R_{sky}(Bouyer 2009). The albedo of the urban surfaces is denoted α.

$$R_{net} = (1-\alpha)\, R_{sun} + R_{IR,Urb\downarrow} + R_{IR,Urb\uparrow} + R_{sky\downarrow} + R_{sky\uparrow} \quad (2)$$

The sky total heat flux is defined as the total net flux exchanged between the sky and the ground's surface. The flux incoming from the sky can either be measured or estimated through correlation involving the outside bulb temperature and/or the air water steam (sky nebulosity) (Martin and Berdahl 1984). The used correlation is described by Eq. (3). It considers that the sky temperature is equal to the outside bulb temperature minus ten degree Celsius (Clus 2007).

$$R_{sky\downarrow} = \sigma\,(T_{air} - 10 + 273.15)^4 \quad (3)$$

Sensible heat flux. It is calculated by multiplying the convective heat transfer coefficient (CHTC) denoted h_c by the difference between the surface (T_{surf}) and the air (T_{air}) temperatures. The evaluation of the CHTC is a tricky point. It can either be deduced by a coupled thermo-aeraulic simulations or estimated through empirical correlations. The first method being expensive in terms of computational cost, correlations are usually used in building energy simulation tools. Those correlations evaluate the CHTC from the wind speed (v_{air}) monitored at the studied surface (Palyvos 2008). Jayamaha, Wijeysundera, and Chou (1996) correlation is used here (Eq. 4).

$$h_c = 5{,}85 + 1{,}7\,v_{air} \quad (4)$$

Runoff sensible heat flux. It is exchanged between the water and the soil surface and estimated by means of the energy absorbed by the water layer as shown in Eq. (5) with ρ the density (kg/m³) and $C_p$the specific heat (J/Kg/K). At the time step t, a water height $h_{w,spr}$ is evenly sprinkled over the surface. The water is assumed at the network temperature (T_w).

$$\boldsymbol{Q_{wat-pav}} = \frac{\boldsymbol{\rho_w\, C_{p,w} h_{w,spr}(t)}}{\boldsymbol{\Delta t}}\,(\boldsymbol{T_{surf}} - \boldsymbol{T_w}) \quad (5)$$

Latent heat flux. It is emitted when a part of the water runoff evaporates. It depends on the amount of water available at the surface and the potential latent heat flux. The latter represents the *evaporative power* of the air (LE_{th}). It can be calculated by the Dalton Equation using the mass-transfer method (Eq. 6) with L the latent heat of the vaporization of water (J/kg). The vapor pressures ($P_{sat}$and P_v) are calculated using the Magnus-Tetens formulas.

$$\boldsymbol{LE_{th}} = \frac{\boldsymbol{h_c\, L}}{\boldsymbol{C_{p,air}}} \cdot [\boldsymbol{P_{sat}}(\boldsymbol{T_{surf}}) - \boldsymbol{P_v}(\boldsymbol{T_{air}})] \quad (6)$$

From the potential latent heat flux, a potential evaporation water height ($h_{evap,th}$) can be calculated as described by Eq. (7).

$$\boldsymbol{h_{evap,th}} = \frac{\boldsymbol{LE_{th}\,\Delta t}}{\boldsymbol{L.\rho_w}} \quad (7)$$

The latent heat flux can then be calculated from the available water height at the surface. If the potential evaporation water height is higher than the available water height, all the water present at the surface evaporates. Otherwise, only a part of the water layer evaporates.

Water height monitoring. At each time step, a water layer can be spread over the surface. The amount of water spreads over the surface is added to the previous one. Part of this water layer can then runoff and part of it can be stored at the surface until it evaporates. The surface water-holding capacity defines which proportion of the water height is stored in the pavement porosity. If the resulting water layer is higher than the pavement water holding capacity, part of the water layer runoffs directly to the sewage. The resulting water layer is then set at the pavement water holding capacity. Three cases are distinguished to calculate the surface energy balance and monitor the water height. Details on the flowchart and the heat fluxes can be found in Azam, Bernard, et al. (2018).

Description of the case study

The model is applied to the Part-Dieu district at Lyon in France (see Fig. 2). The system spreads a thin layer of water over the road pavement surface thanks to sprinklers located in the curbside (see Fig. 2a). It has been tested during three consecutive summer periods from 2012 to 2014, with various watering scenarios. Data from the last and most complete measurement campaign are used here. The soil model is evaluated on two days : the 26th and the 27th of July 2014. Data from the 25th of July are used to initialize the model.

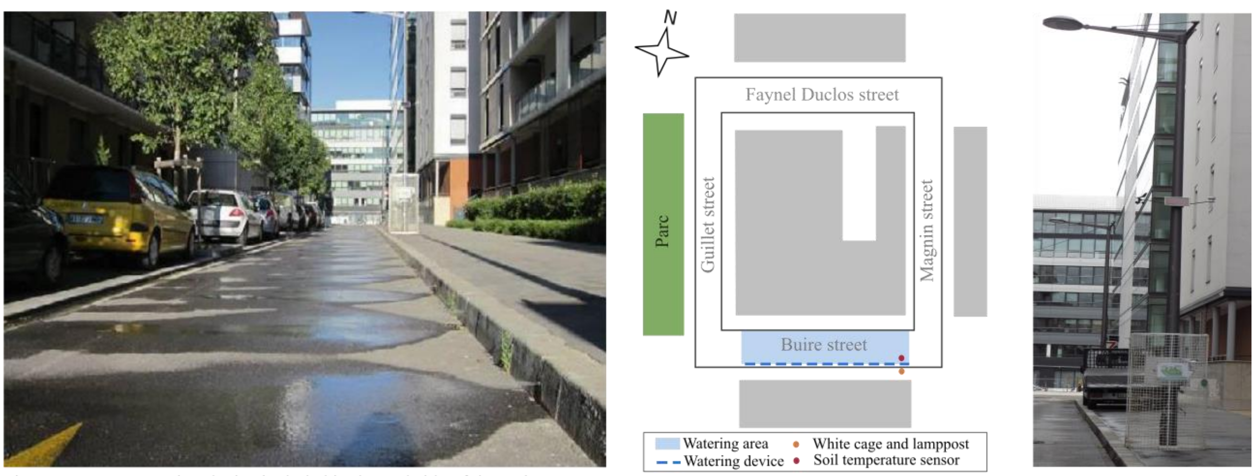

Fig a. Pavement watering device included in the curbside of the Buire street. Fig b. Part Dieu district Fig c. Lamppost

Figure 2. Experimental case study presentation. Wind speed and global horizontal irradiance are measured on the lamppost at a height of 4 m, the air temperature in the white cage at a height of 1.5 m, the soil temperature sensor is located at a depth of 1 cm (Source Veolia 2EI).

Several parameters of the street have been monitored to evaluate the efficiency of the watering events. We focus on the soil temperature, the wind speed, the global horizontal irradiance and the air temperature. The data were collected with a time step of one minute and averaged over 15 minutes.

Data on the events intensity and duration were collected from the *info-climat.fr* website. Six watering events occurred during the 26th and the 27th of July. Events from the 26th of July are natural rain events. At midnight, 5.9 mm water height during 90 minutes is measured. The same day at 13h, 3 mm and at 18h 0.2 mm are measured. On the 27th of July, the watering device was tested from 17:00 to 22:00 (GMT). A thin layer of 0.063 mm on average was spread every 20 minutes on the road surface.

Model setup

The simulations are run from the 25th of July 2014, 00:00 to the 27th of July 2014, 23:45 with a time step of 15 minutes. The surface characteristics of the urban scene have not been measured. Surface composition, layer thickness and thermal characteristics are assumed. Theoretical composition of the road and sidewalk of the Buire street are known, but the thermal properties have not been measured. We defined them using data measured on similar materials (Pilate, O. 2006). They are presented in table 2. The albedo of the buildings walls, roofs and urban soils have been set respectively to 0.54, 0.40, 0.17 and the emissivity to 0.90, 0.90, 0.95. The road water-holding capacity have not been measured either. It has been set to 0.8 mm using data from a parking lot with similar pavement characteristics (Azam, Bernard, et al. 2018).

Table 2. Soil thermal characteristics defined from Pilate, O. (2006)

Surface	Layer	layer thickness (m)	conductivity (W/mK)	specific heat (J/kgK)	density (kg/m3)
Buire Road	very thin asphalt concrete	0.03	2.0	869	2350
	thick solution system	0.07	2.0	869	2142
	"as dug" gravel	0.08	0.52	838	1703
	Asphalt	0.08	2.0	869	2350
	"as dug" gravel (GNT031)	0.10	0.52	838	1703
	"as dug" gravel (GNT080)	0.50	0.89	837	1750
Buire Sidewalks	Very thin asphalt concrete	0.02	0.7	920	2120
	Concrete	0.10	1.51	880	2200
	"as dug" gravel (GNT031)	0.08	0.52	838	1703
	"as dug" gravel (GNT080)	0.50	0.89	837	1750
Building	Concrete	0.20	1.75	1000	2300
	Insulation	0.15	0.04	1030	30

Methodology and assessment procedure

The ability of the model to reproduce the physical phenomena involved is first evaluated using data measured locally by Veolia 2EI for the air temperature and wind speed. This first scenario will be defined as the reference one.

As designers usually do not have access to local weather data but use data from meteorological site, the results of the reference scenario will be compared to various scenario using data from Vaulx-en-Velin meteorological site for the air temperature and the wind speed. One input parameter is modified at a time for simulation 2 and 3. Simulation 4 studies the combined effect. Table 3 sums up the origin of the input data used for each simulation scenario. The root-mean-square error between the soil temperatures at a depth of 1 cm (where a sensor has been put by Veolia 2EI) is used to compare the simulation results.

Finally, in order to quantify the impact of watering on the surface temperature. The surface temperature with and without watering are compared for the Buire street.

Table 3. Simulation scenarios definition

Scenario	Simulation 1	Simulation 2	Simulation 3	Simulation 4
Air temperature	Buire	Buire	Vaulx-en-Velin	Vaulx-en-Velin
Wind speed	Buire	Vaulx-en-Velin	Buire	Vaulx-en-Velin

Results and discussions

Comparison between simulations and measurements

First, the model ability to reproduce the physical phenomenas evaluated using local data. Fig. (3) presents the evolution of the temperature measured and calculated at a depth of 1 cm in the soil. The model mainly under-estimates the surface temperature for the 26th and the 27th of July during the night. During the 27th of July afternoon (14:00-16:00), the surface temperature is overestimated. The RMSE error between the two curves is of 2.99 °C. Each source of uncertainty that could explain this error is discussed hereafter. The first point investigated is the global horizontal irradiance. Fig. 4 compares the global irradiance measured by Veolia 2EI and the one calculated by SOLENE. Results of the simulation are given for a triangle located on the soil as close as possible to the temperature sensor. The global horizontal irradiance has been measured at a height of 4 m. Despite the altimeter difference, the dynamic of the radiation is respected. The street is lighted at the beginning of the day (5h-6h30) and during the afternoon (14:00-16:00). For both curves, sunrise and sunset occurred simultaneously. During the day, the heat flux measured is higher than the one calculated, on the contrary, during the afternoon, the simulation overestimates this heat flux. An error of 72.79 W/m² (RMSE) has been calculated between the two curves. Those differences could explain part of the surface temperature underestimation during the day from 5h to 14h and overestimation at the end of the afternoon between 14h and 16h. Another point could be the sky total heat flux. Meteorological data were not available to estimate it precisely at the meteorological station. Among the correlations found to model the sky radiative heat flux, large differences are observed (Clus 2007). Therefore, the sky heat flux has an important uncertainty, as sky temperature has an uncertainty of ±10 °C.

As cited before, the soil composition is not known with accuracy. It will definitely have a large impact on the conductive heat flux. The number of layers and the few measurements made it impossible to calibrate the soil properties.

The runoff sensible heat flux depends on the pavement water holding capacity and the spread water temperature. This last parameter has not been monitored. An hypothesis is then made on the network temperature.The surface state (dry or wet) has not been monitored neither the sewage heat flow. As a consequence, the water holding capacity of the pavement can not be calibrated. Finally, the sensible heat flux depends on the CHTC, which depends on the correlation used. Here, the choice was made to use a linear equation lying on the local wind speed. In order to improve the estimation of the sensible heat flux, a coupled simulation could be done to obtain local wind velocities.

Two others parameters affect the sensible heat fluxes calculation, the air temperature and wind speed. Here local data are used. Yet, they are not always available.

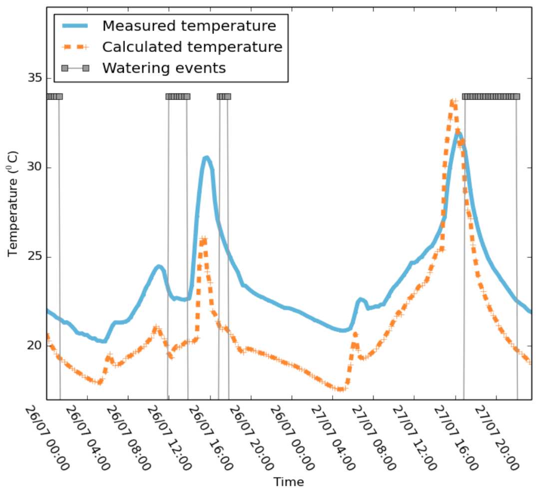

Figure 3. Comparison of the measured temperature at a depth of 1 cm and the one simulated using scenario 1.

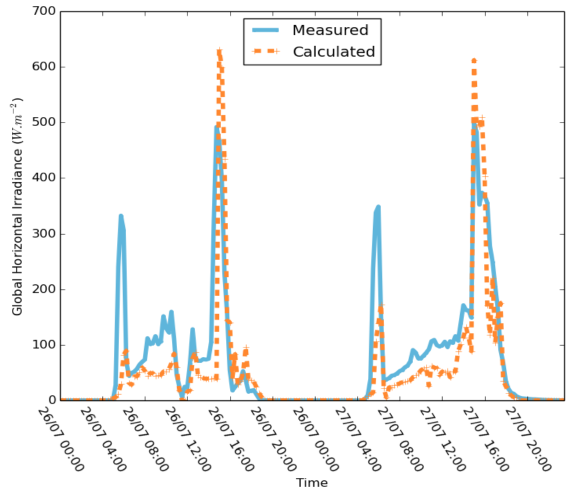

Figure 4. Comparison of the global horizontal irradiance calculated and measured in the street.

Sensitivity analyses: impact of using non-local data

In this second part, we aim at quantifying the impact of using non-local data for the air temperature and the wind speed. First, the input data are compared, then their effect on the soil temperature is studied. Results of the four simulations are compared.

Input data comparison. Usually the air temperature comes from an operational measure station (at an airport for example) which can be far away from the studied district.Fig. (5) shows the local data measured in the studied street by Veolia 2EI and the one from Vaulx-en-Velin operational weather station (7 km distant). During the night, the meteorological station temperature are lower than the air temperature measured in the street, what clearly denotes a UHI effect. A RMSE of 1.89 °C can be observed between the two curves.

Similarly, wind velocity measured from the meteorological station is not representative of the one observed in the street. For the calculation CHTC, the local wind speed is needed. In order to estimate precisely this wind speed using the given meteorological wind speed and direction, a coupled thermo-aeraulic simulation can be done. As it has a very large computation cost, this option is not considered here but we will assess the impact it would have.

Meteorological data from the Vaulx-en-velin site has been analysed to defined the site principal wind direction and intensity. For the 26th of July, three main directions can be observed: West, North-North-East, West-South-West. For the 27th of July, the main direction is North. Consequently, aeraulic simulations have been launched for three directions: North (10°), East (67.5°), West (280°) and 7 intensities from 0.1 to 5.5 m/s. Results from the North (10°) direction are used when the wind direction is included in the segments (0°,45°) and (320°, 360°),the East direction for the segment (45°, 180°) and the West direction for the segment (180°, 320°).

Three wind speed curves are compared in Fig. (6) : the measurement in the Buire street by Veolia 2EI, the measurement at Vaulx-en-velin station and the estimation from the aeraulic simulation (Saturne model). During the nights, the local wind speed was below the anemometer release speed. At the Vaulx-en-Velin station, the wind intensity is also higher during the daytime than during the night. However, the intensity is generally above the one measured locally. For the 27th of July, the estimated wind speed is close to the measurement during the daytime. Indeed, the direction selected to execute the aeraulic simulations are in good agreement with the wind rose principal direction. However, for the 26th of July, more directions would have been necessary to represent the direction in the segment (90, 270). The calculation overestimates the local wind speed.

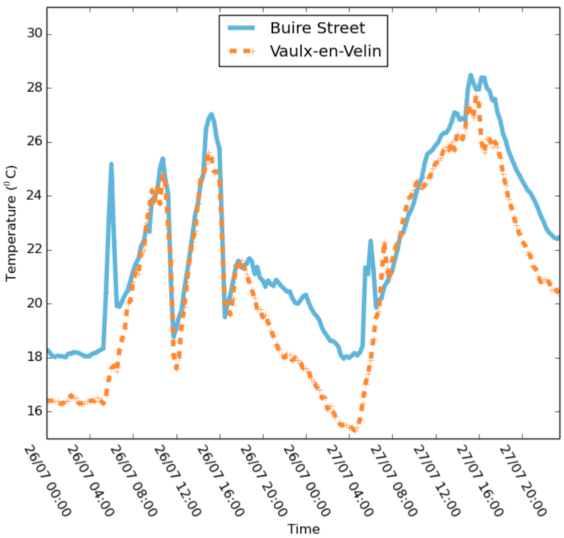

Figure 5. Comparison of the air temperature measured in the street and at the meteorological station Vaulx-en-Velin.

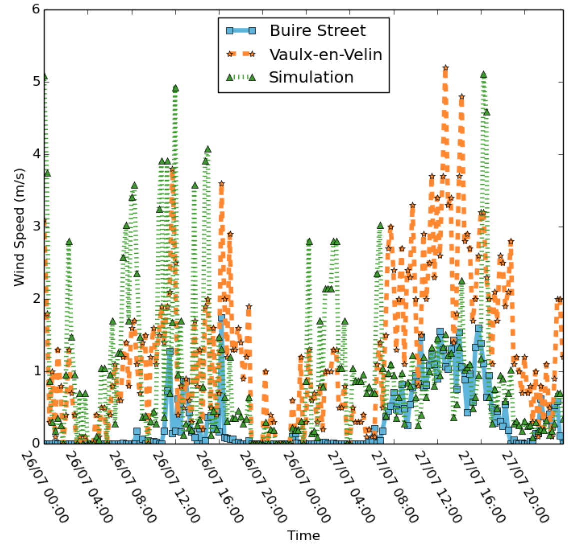

Figure 6. Comparison of the wind speed measured in the street, the one measured at the Vaulx-en-Velin site and the one estimated from the aeraulic simulations

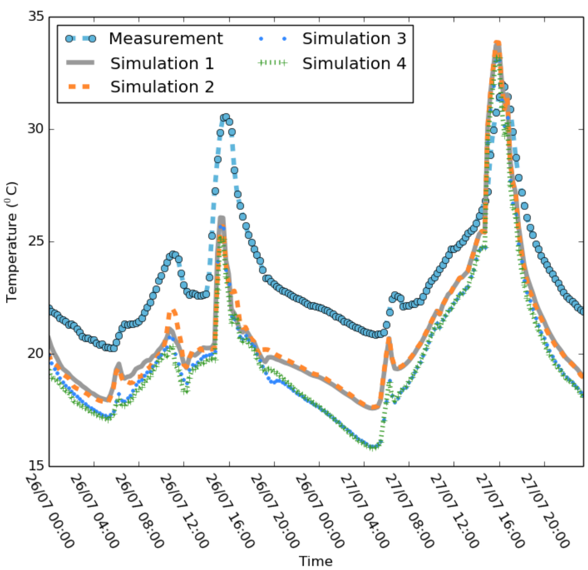

Figure 9. Comparison of the soil temperature calculated for the four scenarios and the measured one.

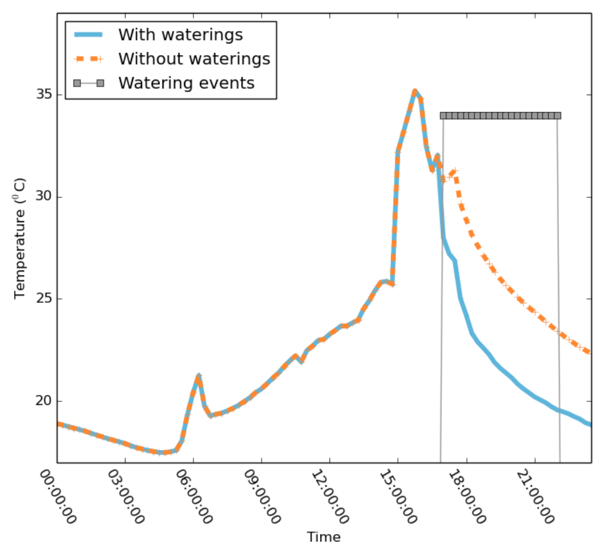

Figure 10. Comparison of the soil surface temperature calculated with and without watering for the 27th of July.

Influence on the soil temperature. The impact of using non-local data on the soil temperature calculation is studied. Fig. (9) shows the results of the four simulated scenarios (see table 3). Errors between the several curves are summarized in table 4.

Table 4. RMSE using local and non-local data (temperature at a depth of 1cm).

	Simulation 1	Simulation 2	Simulation 3	Simulation 4
Measurements	2.99	2.99	3.75	3.75
Simulation 1	-	0.27	0.93	0.87

Simulation 3 uses non-local air temperature and local wind speed. Using non-local air temperature has a high impact on the soil temperature. The error calculated between this simulation and the reference simulation reaches 0.93 °C. However, if we consider using non-local wind speed (Simulation 2), the error with the reference simulation reaches only 0.27 °C. Considering the local air temperature (UHI effect), the street surface temperature is more accurate.

Simulation 4 considers the combined effects of taking into account non-local data for both the air temperature and the wind speed. During the nighttime, the resulting errors cancel out. Curve of simulation 4 exceeds curve of simulation 3.

Influence of the watering scenario on the surface temperature

The influence of the watering on the pavement temperature is now assessed. Results of simulation 1 are compared to the results of a simulation with the same input conditions but without evening watering. As soon as water has been spread over the surface, the temperature drops (Fig. (10)). The surface cooling persists during the whole event. It decreases the surface temperature by 4.09 °C (RMSE calculated from 17:00 to 00:00), with a maximal difference of 4.81 °C.

Due to the East-West orientation of the street, the impact of the watering from 17:00 to 22:00 is limited. It would have been higher if the watering scenario was synchronized with the street irradiance.

Conclusion

The pavement watering model has been applied under urban conditions. The RMSE of 2.99 °C between the soil temperature measurements and the calculation highlights the difficulties to reproduce such conditions. A coupled heat and mass transfer soil model could have improved the results dynamics. However, whatever the level of detail of the soil model used, we face up the reality of lacking information: thermal materials characteristics, pavement water holding capacity, sky total heat flux...

In a second part, the influence of using non-local climate input data has been investigated. The air temperature had more influence on the soil temperature than the wind speed. These results show the impact of the UHI on the surface temperature. Having the local air temperature is an important challenge to improve the simulation results.

Finally, the impact of an evening watering scenario has been quantified. Results of the simulation show that the surface temperature can be reduced by 4.09 °C with such a watering scenario and bring to light the fact that this model can be used to assess the cooling effect of waterings at micro-scale.

The efficiency of this mitigation technique is constrained by the potential evaporation of the surface. It depends mainly on two parameters, the surface energy balance and the surface characteristics. For the first parameters, a watering scenario could be optimized based on the global horizontal irradiance and CHTC. For the second parameters, the characterization of the water holding capacity of the surface would permit to optimize the water layer spread over the surface to maximized evaporation and minimize water use.

Acknowledgments

The first part and this work was conducted within the framework of the EVA project funded by the ADEME under contract 1216C0037. We acknowledge Veolia 2EI that in the frame of this contract shared their measurement data.

References

Azam, Marie-Hélène, Jérémy Bernard, Benjamin Morille, Marjorie Musy, and Hervé Andrieu. 2018. « A pavement-watering thermal model for SOLENE-microclimat: Development and evaluation ». *Urban Climate* 25: 22-36. https://doi.org/10.1016/j.uclim.2018.04.005.

Azam, Marie-Hélène, Benjamin Morille, Jérémy Bernard, Marjorie Musy, and Fabrice Rodriguez. 2018. « A new urban soil model for SOLENE-microclimat: Review, sensitivity analysis and validation on a car park ». *Urban Climate* 24 (juin): 728-46. https://doi.org/10.1016/j.uclim.2017.08.010.

Bouyer, Julien. 2009. « Modélisation et simulation des microclimats urbains-Étude de l'impact de l'aménagement urbain sur les consommations énergétiques des bâtiments ». Université de Nantes.

Broadbent, Ashley M., Andrew M. Coutts, Nigel J. Tapper, and Matthias Demuzere. 2017. « The cooling effect of irrigation on urban microclimate during heatwave conditions ». *Urban Climate*, mai. https://doi.org/10.1016/j.uclim.2017.05.002.

Clus, Owen. 2007. « Condenseurs radiatifs de la vapeur d'eau atmosphérique (rosée) comme source alternative d'eau douce ». Phdthesis, Université Pascal Paoli. https://tel.archives-ouvertes.fr/tel-00320450/document.

Hendel, Martin, and Laurent Royon. 2015. « The Effect of Pavement-Watering on Subsurface Pavement Temperatures ». *Urban Climate* 14 (décembre): 650-54. https://doi.org/10.1016/j.uclim.2015.10.006.

Jayamaha, S. E. G., N. E. Wijeysundera, and S. K. Chou. 1996. « Measurement of the heat transfer coefficient for walls ». *Building and Environment* 31 (5): 399-407. https://doi.org/10.1016/0360-1323(96)00014-5.

Martin, Marlo, and Paul Berdahl. 1984. « Characteristics of infrared sky radiation in the United States ». *Solar Energy* 33 (3): 321-36. https://doi.org/10.1016/0038-092X(84)90162-2.

Palyvos, J.A. 2008. « A Survey of Wind Convection Coefficient Correlations for Building Envelope Energy Systems' Modeling ». *Applied Thermal Engineering* 28 (8-9): 801-8. https://doi.org/10.1016/j.applthermaleng.2007.12.005.

Pilate, O. (2006). Evolution de la température d'une... - Google Scholar ». s. d. Consulté le 10 avril 2019. https://scholar.google.fr/scholar?hl=fr&as_sdt=0%2C5&q=Pilate%2C+O.+%282006%29.+Evolution+de+la+temp%C3%A9rature+d%27une+couche+d%27enrob%C3%A9+bitumineux+nouvellement+pos%C3%A9e.+Compte+rendu+de+recherche+C.+R.+R.&btnG

Takahashi, R., A. Asakura, K. Koike, S. Himeno, and S. Fujita. 2010. « Using snow melting pipes to verify the water sprinkling's effect over a wide area. Sustainable techniques and strategies in urban water management ». In *7th International Conference. Lyon, France, Novatech*.